Journal of Physics: Conference Series **455** (2013) 012018 doi:10.1088/1742-6596/455/1/012018

Production of beauty and quarkonia in ATLAS

T Jakoubek on behalf of the ATLAS Collaboration

Faculty of Nuclear Sciences and Physical Engineering, Czech Technical University in Prague, Brehova 7, Prague, Czech Republic

E-mail: tomas.jakoubek@cern.ch

Abstract. Quarkonia and b-hadron production cross sections were measured using the ATLAS detector in proton-proton collisions at the Large Hadron Collider at $\sqrt{s} = 7$ TeV using data collected in 2010 and 2011 runs. The new bottomonium state $\chi_b(3P)$ has been observed.

1. Introduction

Quarkonia (bound states of a quark and its anti-quark) and other particles containing heavy quarks provide a good ground for testing the validity of quantum chromodynamics (QCD). Quarkonia production mechanisms are still not well understood. Several models (Colour Singlet and Colour Octet production mechanisms) describe the transverse momentum (p_{T}) spectra and production cross sections observed at the Tevatron, but polarization predictions are not in agreement with measurements. The b-hadron production cross section has been predicted with next-to-leading-order (NLO) accuracy and several measurements were performed at the Sp$\overline{\mathrm{p}}$S and the Tevatron colliders. Theory predictions and measurements are in a good agreement, but they still have large uncertainties. The Large Hadron Collider (LHC) opens a new region of energies for all these studies.

2. The ATLAS detector

The ATLAS experiment [1] is a multipurpose particle physics detector at the LHC, optimized for high p_{T} physics and instantaneous luminosity up to 10^{34} cm^{-2}·s^{-1}. The detector has forward-backward symmetric cylindrical geometry with almost 4π coverage. Precise tracking is provided by its innermost part, the Inner Detector (ID), which consists of a silicon pixel detector, a silicon microstrip detector and a transition radiation tracker, all immersed in a 2 T axial magnetic field. The ID covers the pseudorapidity region of $|\eta| < 2.5$ and is enclosed by the electromagnetic and hadronic calorimeters. The outermost part of the ATLAS detector is the Muon Spectrometer (MS). It covers the pseudorapidity in the interval of $|\eta| < 2.7$ and is located within the magnetic field produced by three large superconducting air-core toroid systems.

The ATLAS detector uses a three-level trigger system (hardware-based Level 1 and software-based Level 2 and Event Filter), which reduces the event rate from 20 MHz to several hundred Hz. The triggers used in the analyses presented rely on the Minimum Bias Trigger Scintillators (MBTS) and the muon trigger chambers. During the later periods of 2010 data taking with higher instantaneous luminosity, selective muon triggers with high p_{T} threshold (4, 6 or 10 GeV/c) were required.

3. Measurement of the J/ψ production

The J/ψ meson is perhaps the best known state of charmonium, the bound state of $c\overline{c}$ quarks. This meson was discovered in the 1970s and since then its properties have been deeply studied. Thus it can be used not only for heavy quark studies, but also for calibration of the high-energy physics detectors.

The J/ψ double differential production cross-section was measured [2] in bins of p_{T} and rapidity y on the ATLAS detector using data from 2010 proton-proton 7 TeV collisions with integrated luminosity of 2.2 pb^{-1}. The differential cross-section was measured as

$$\frac{\mathrm{d}^2\sigma(J/\psi)}{\mathrm{d}p_{\mathrm{T}}\mathrm{d}y}\mathrm{Br}(J/\psi \to \mu^-\mu^+) = \frac{N^{J/\psi}_{\mathrm{corr}}}{\mathcal{L}\cdot\Delta p_{\mathrm{T}}\Delta y}, \tag{1}$$

where $N^{J/\psi}_{\mathrm{corr}}$ is the J/ψ yield in a given $p_{\mathrm{T}} - y$ bin after continuum background subtraction and correction for detector efficiency, bin migration and acceptance effects, $\mathcal{L}$ is the integrated luminosity of the data sample and Δp_{T} and Δy are the p_{T} and rapidity bin widths respectively. In order to obtain the true number of J/ψ s every candidate was weighted by:

$$w^{-1} = \mathcal{A}\cdot\mathcal{M}\cdot\epsilon^2_{\mathrm{trk}}\cdot\epsilon^-_\mu(p^-_{\mathrm{T}},\eta^-)\cdot\epsilon^+_\mu(p^+_{\mathrm{T}},\eta^+)\cdot\epsilon_{\mathrm{trig}}, \tag{2}$$

where $\mathcal{A}$ is the kinematic acceptance, describing the probability of the muons from a J/ψ falling into the fiducial volume of the detector. $\mathcal{M}$ is the correction factor for bin migrations due to the finite detector resolution, ϵ_{trk} is the ID tracking efficiency, $\epsilon^\pm_\mu$ is the single-muon offline reconstruction efficiency and ϵ_{trig} is the trigger efficiency. The acceptance $\mathcal{A}$ depends on the p_{T} and y of the J/ψ candidate and also on its spin-alignment, which is not yet known for the LHC conditions. Five extreme cases can be identified in the general parametrization of the angular distribution and these were used to calculate the maximal variation of the acceptance. The central values were obtained using the hypothesis with flat polarization. The kinematic acceptance was calculated using generator-level Monte Carlo.

The total inclusive cross-section for a J/ψ produced within $|y| < 2.4$ and $p_{\mathrm{T}} > 7$ GeV, multiplied by the branching fraction into muons, has been measured to be:

$$Br(J/\psi \to \mu^+\mu^-)\sigma(pp \to J/\psi X) = 81 \pm 1\,(\mathrm{stat.}) \pm 10\,(\mathrm{syst.}) \pm^{25}_{20}\,(\mathrm{spin}) \pm 3\,(\mathrm{lumi.})\ \mathrm{nb}. \tag{3}$$

3.1. Measurement of the non-prompt J/ψ fraction

The J/ψ mesons can be produced directly in pp collision, moreover they can originate from decays of heavier charmonium states or from the decay of a B-hadron (non-prompt production). As B-hadrons are long-lived, the pseudo-proper lifetime can be used as a discriminating factor between prompt and non-prompt production. It is defined as:

$$\tau = \frac{L_{xy}\cdot m^{J/\psi}_{\mathrm{PDG}}}{p^{J/\psi}_{\mathrm{T}}} \tag{4}$$

where L_{xy} is the vertex distance projected onto the transverse momentum direction, $m^{J/\psi}_{\mathrm{PDG}}$ is the world average value of the J/ψ mass and $p^{J/\psi}_{\mathrm{T}}$ is the transverse momentum of the J/ψ candidate. The fraction of prompt and non-prompt J/ψ production as a function of p_{T} was determined using a simultaneous fit of mass and pseudo-proper lifetime in four y bins. The results, together with CDF and CMS measurements for comparison, are shown in Fig. 1.

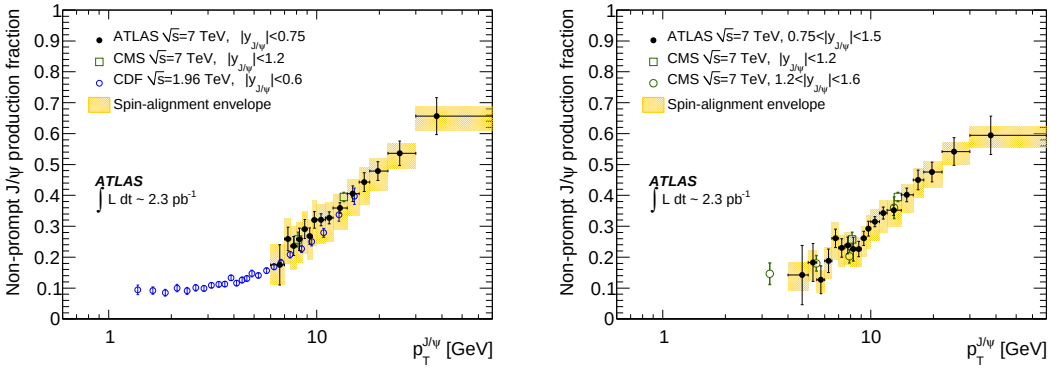

Figure 1. The non-prompt to prompt J/ψ fraction as the function of p_{T} in the first two rapidity bins. The yellow band represents the variation of the result under various spin-alignment scenarios. The equivalent results from CMS and CDF are included. [2]

3.2. The prompt and non-prompt differential production cross-section

The prompt J/ψ fraction was also used to derive the prompt and non-prompt J/ψ production cross-sections from the inclusive production cross-section. The total production cross-section for non-prompt J/ψ within $|y| < 2.4$ and $p_{\mathrm{T}} > 7$ GeV, multiplied by the branching fraction into muons, has been measured to be:

$$\begin{aligned} &Br(J/\psi \to \mu^+\mu^-)\sigma(pp \to B + X \to J/\psi + X') = \\ &= 23.0 \pm 0.6(\mathrm{stat.}) \pm 2.8(\mathrm{syst.}) \pm 0.2(\mathrm{spin}) \pm 0.8(\mathrm{lumi.})\ \mathrm{nb}. \end{aligned} \quad (5)$$

Results were compared to Fixed Order Next-to-Leading Logarithm (FONLL) calculations [6]. This comparison is shown in Fig. 2, where a good agreement between the experimental data and the theoretical prediction can be seen. The total integrated prompt J/ψ production cross-section within $|y| < 2.4$ and $p_{\mathrm{T}} > 7$ GeV, multiplied by the branching fraction into muons, has been measured to be:

$$Br(J/\psi \to \mu^+\mu^-)\sigma(pp \to \text{prompt } J/\psi X) = 59 \pm 1\,(\mathrm{stat.}) \pm 8\,(\mathrm{syst.}) \pm {}^{9}_{6}\,(\mathrm{spin}) \pm 2\,(\mathrm{lumi.})\ \mathrm{nb}. \quad (6)$$

Comparison with the predictions of the Colour Evaporation Model (CEM) [7, 8, 14] and the Colour Singlet Model (CSM) [9, 10] at next-to-leading order (NLO) and partial next-to-next-leading order (NNLO*) calculations is shown in Fig. 3. One can see that contributions from CSM NNLO* show better agreement than the ones from NLO. The shape of the CEM predictions does not provide a good description.

4. Measurement of the Υ production

Production cross-section measurement of the bottomonium states Υ(1S, 2S, 3S) in the di-muon decay mode has been done similarly as the cross-section of the J/ψ in bins of p_{T} and y [3]. To remove the uncertainty due to spin-alignment, this measurement was performed in the ATLAS fiducial region with $p_{\mathrm{T}}^{\mu} > 4$ GeV and $|\eta^{\mu}| < 2.3$. Data from 2011 proton-proton 7 TeV LHC collisions were used with integrated luminosity of 1.8 fb^{-1}. The mass difference was used to separate the three bottomonium states. The number of Υs was then determined using an unbinned maximum likelihood fit to the di-muon invariant mass distribution. Corrected cross-sections integrated over p_{T} and y bins are shown in table 1. Differential cross-sections multiplied by the di-muon branching fraction of Υ(1S) production were extrapolated to the full phase space

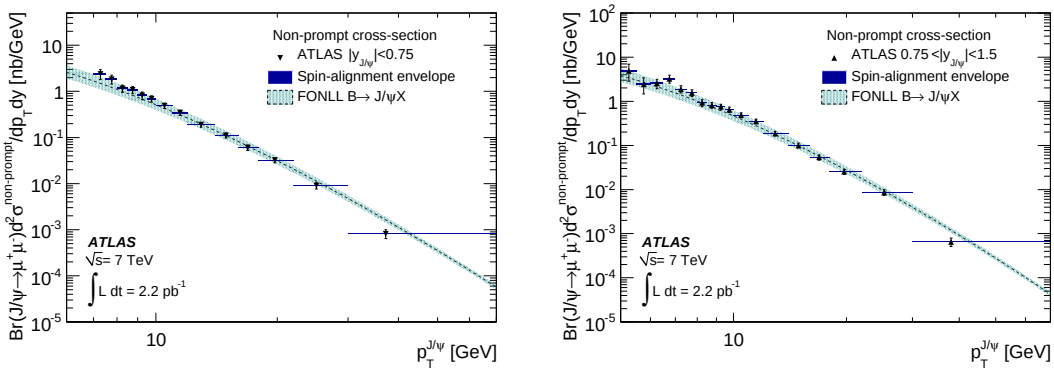

Figure 2. The non-prompt J/ψ production cross-section as the function of p_{T} in the first two rapidity bins, compared with the predictions of FONLL theory. The blue band represents spin-alignment uncertainty. [2]

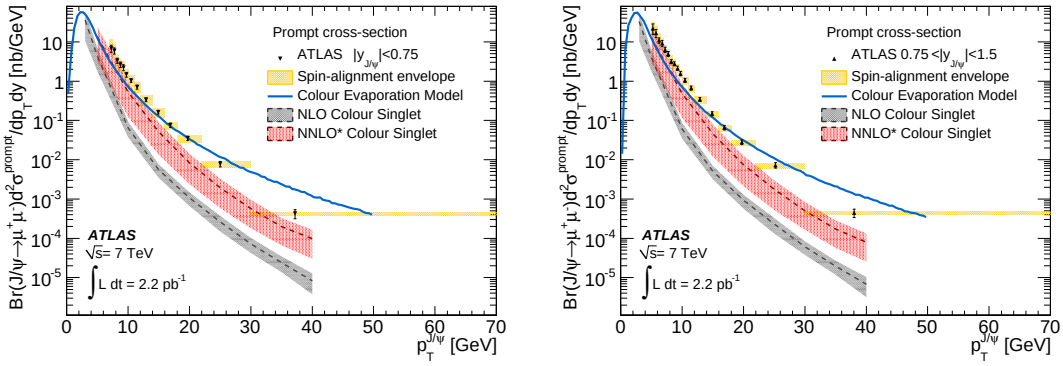

Figure 3. The prompt J/ψ production cross-section as the function of p_{T} in the first two rapidity bins. The yellow band represents spin-alignment uncertainty. Predictions from NLO and NNLO* calculations, and the Colour Evaporation Model are also shown. [2]

Table 1. Corrected cross-section measurements in the range $p_{\mathrm{T}}^{\Upsilon} < 70$ GeV and $|y^{\Upsilon}| < 2.25$. [3]

State	$\sigma(pp \to \Upsilon)Br(\Upsilon \to \mu^+\mu^-)$
Υ (1S)	8.01 $\pm$ 0.02 (stat.) $\pm$ 0.36 (syst.) $\pm$ 0.31 (lumi.) nb
Υ (2S)	2.05 $\pm$ 0.01 (stat.) $\pm$ 0.12 (syst.) $\pm$ 0.08 (lumi.) nb
Υ (3S)	0.92 $\pm$ 0.01 (stat.) $\pm$ 0.07 (syst.) $\pm$ 0.04 (lumi.) nb

of produced Υ mesons and compared to the NNLO* CSM [10–12] and CEM [7,13,14] predictions. These comparisons are shown in Fig. 4. CSM underestimates the data in bins of higher p_{T}, while CEM predictions show a better match with the data at higher p_{T}, but have difficulties with modelling the shape of the spectrum at lower p_{T}. The ratio of Υ(2S) and Υ(3S) cross-sections over Υ(1S) cross-section was also determined. It is flat across the full rapidity interval, as can be seen in Fig. 5 (left). In p_{T} it steadily rises and saturates above the value in the range

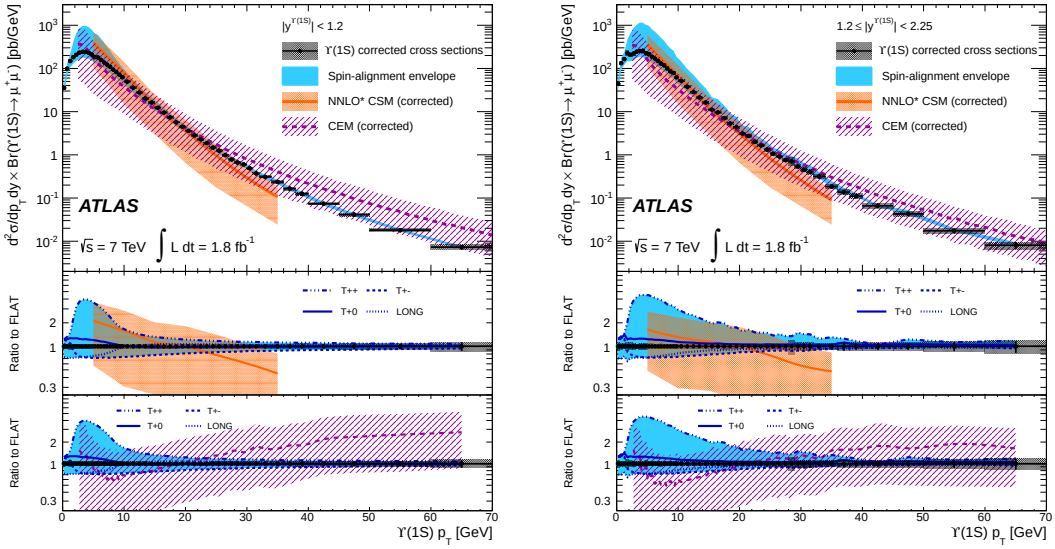

Figure 4. The differential $\Upsilon(1S)$ cross-sections multiplied by corresponding the di-muon branching fraction extrapolated to the full phase space in two rapidity bins. The blue band represents the spin-alignment uncertainty. Predictions of the NNLO* CSM and CEM are also shown. The ratios of these predictions to the measured cross-sections are in the lower panes for CEM (middle) and CSM (bottom). [3]

30-40 GeV/c, where the direct production dominates (see Fig. 5 middle and right). However, the measured values are higher than theory predictions.

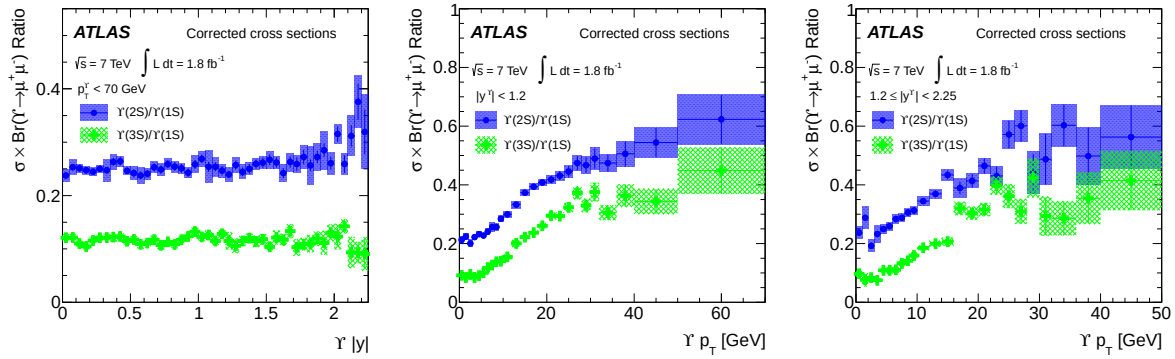

Figure 5. The ratios of the $\Upsilon(2S)$ /$\Upsilon(1S)$ and $\Upsilon(3S)$ /$\Upsilon(1S)$ cross-section as a function of di-muon rapidity (left) and di-muon p_{T} (middle and right). Error bars do not include spin-alignment effects. [3]

5. Observation of the new χ_b(3P) states

A new quarkonium state has been observed [4] in radiative transitions to the $\Upsilon(1S)$ and $\Upsilon(2S)$ in the ATLAS measurements in 2011 proton-proton 7 TeV collisions with integrated luminosity of 4.4 fb^{-1}. Υ(1S, 2S) then decays into a $\mu^+\mu^-$ pair and the photon is reconstructed either through conversion to e^+e^- pair (converted photons) or by the direct calorimetric measurement

(unconverted photons). States χ_b(1P) and χ_b(2P) have already been observed, but the existence of the third bottomonium state χ_b(3P) was only predicted. The invariant mass distribution of di-muon plus photon candidates is shown in Fig. 6. The Υ(1S) mass window was set to be $9.25 < m(\mu\mu) < 9.65$ GeV and for Υ(2S) to be $9.80 < m(\mu\mu) < 10.10$ GeV. An unbinned maximum likelihood fit was performed in order to obtain the three mean values $m_{n=1,2,3}$, where m_3 is an estimate of the mass barycenter of the observed χ_b(3P) signal multiplet:

$$m_3(\text{unconverted photons}) = 10.541 \pm 0.011(\text{stat.}) \pm 0.030(\text{syst.}) \text{ GeV}, \quad (7)$$

$$m_3(\text{converted photons}) = 10.530 \pm 0.005(\text{stat.}) \pm 0.009(\text{syst.}) \text{ GeV}. \quad (8)$$

Due to the substantially smaller systematic uncertainties in the conversion measurement, the value (8) has been chosen as the final result of the new χ_b(3P) state mass.

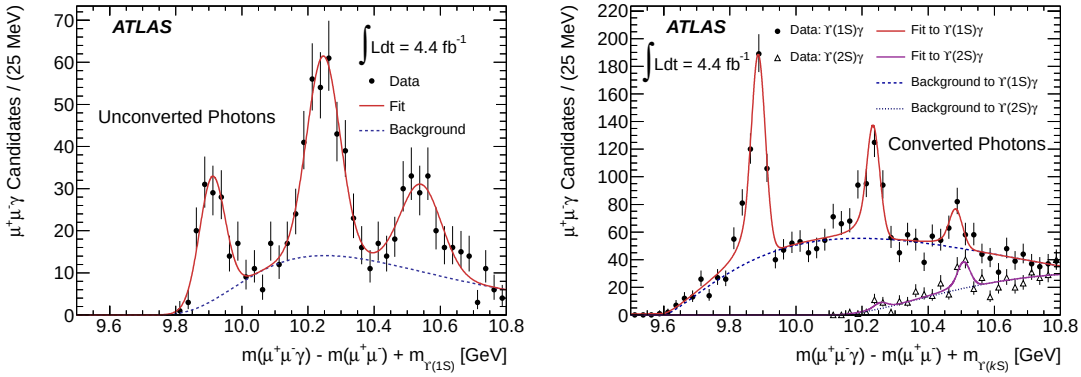

Figure 6. The invariant mass distribution of the $\chi_b \to \Upsilon + \gamma$ candidates for unconverted (left) and converted (right) photons. [4]

6. Measurement of the b-hadron production cross section

The b-hadron (H_b) production cross-section has been measured [5] using partially reconstructed $D^{*\pm}\mu^{\mp}X$ final states. The muon in this case acts as a trigger and the decay of the D meson can be fully reconstructed in the ATLAS detector ($D^{*\pm} \to D^0\pi^{\pm}; D^0 \to \pi K$). For this purpose, 3.3 pb^{-1} of integrated luminosity of 2010 proton-proton 7 TeV ATLAS run have been used. The differential cross-section as a function of p_{T} and pseudorapidity together with the theoretical predictions is shown in Fig. 7. NLO QCD [15–18] calculations underestimate the measured data, but are still consistent within the experimental and theoretical uncertainties. The integrated production cross section for $p_{\mathrm{T}} > 9$ GeV and $|\eta| < 2.5$ was measured to be

$$\sigma(pp \to H_b X) = 32.7 \pm 0.8\,(\text{stat.}) \pm 3.1\,(\text{syst.})^{+2.1}_{-5.6}\,(\alpha) \pm 2.3\,(Br) \pm 1.1\,(\text{lumi.})\ \mu\text{b}, \quad (9)$$

where α stands for the acceptance contribution.

7. Conclusions

The ATLAS experiment has produced impressive and competitive results in Onia and b-hadron measurements. This includes measurement of production cross-sections of prompt and non-prompt J/ψs and b-hadrons. Especially in the case of Υ(1S, 2S, 3S) also production ratios between them have been estimated. In radiative transitions to bottomonium states a new χ_b(3P) state has been observed. All these results will help to improve our understanding of quarkonium production and dynamics.

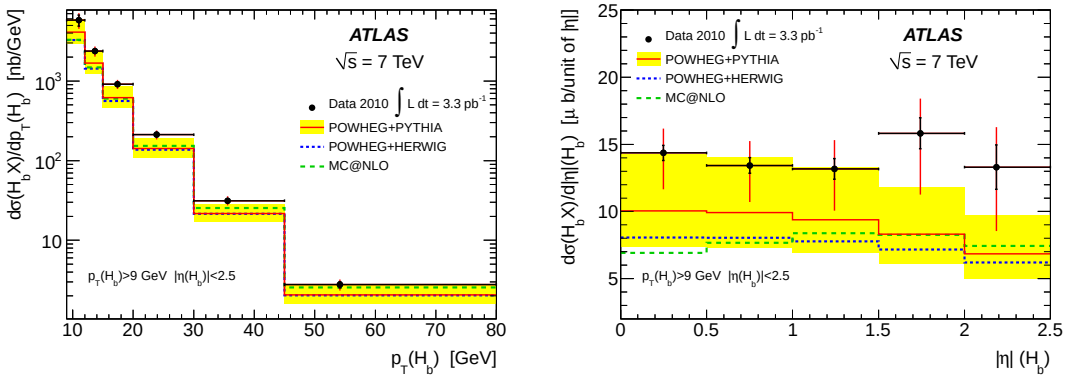

Figure 7. The differential cross section for b-hadron production as a function of p_{T} (left) and $|\eta|$ (right). The comparison with the theoretical predictions is also shown. The inner error bars of the data points represent statistical uncertainties, the outer statistical+total systematic uncertainties. [5]

References

[1] ATLAS Collaboration 2008 *JINST* **3** S08003
[2] ATLAS Collaboration 2011 *Nucl. Phys.* B **850** 387
[3] ATLAS Collaboration 2013 *Phys. Rev.* D **87** 052004
[4] ATLAS Collaboration 2012 *Phys. Rev. Lett.* **108** 152001
[5] ATLAS Collaboration 2012 *Nucl. Phys.* B **864** 341
[6] Cacciari M, Greco M and Nason P 1998 *JHEP* **9805** 007
Cacciari M, Greco M and Nason P 2001 *JHEP* **0103** 006
[7] Ullrich T, Frawley A D and Vogt R 2008 *Phys. Rept.* **462** 125
[8] Barger V D, Keung W Y and Phillips R J N 1980 *Z. Phys.* C **6** 169
[9] Lansberg J P 2010 Total J/ψ production cross section at the LHC (*Preprint* hep-ph/1006.2750)
Brodsky S J and Lansberg J P 2010 *Phys. Rev.* D **81** 051502(R)
[10] Lansberg J P 2009 *Eur. Phys. J.* C **61** 693
[11] Owens J F, Reya E and Gluck M 1978 *Phys. Rev.* D **18** 1501
Kartvelishvili V G, Likhoded A K and Slabospitsky S R 1978 *Sov. J. Nucl. Phys.* **28** 678
Chang C H 1980 *Nucl. Phys.* B **172** 425
Berger E L and Jones D L 1981 *Phys. Rev.* D **23** 1521
Baier R and Ruckl R 1982 *Nucl. Phys.* B **201** 1
Baier R and Ruckl R 1983 *Z. Phys.* C **19** 251
[12] Artoisenet P, Campbell J M, Lansberg J P, Maltoni F and Tramontano F 2008 *Phys. Rev. Lett.* **101** 152001
[13] Fritzsch H 1977 *Phys. Lett.* B **67** 217
Halzen F 1977 *Phys. Lett.* B **69** 105
Gluck M, Owens J F and Reya E 1978 *Phys. Rev.* D **17** 2324
Amundson J F, Eboli O J P, Gregores E M and Halzen F 1996 *Phys. Lett.* B **372** 127
Amundson J F, Eboli O J P, Gregores E M and Halzen F 1997 *Phys. Lett.* B **390** 323
[14] Barger V D, Keung W Y and Phillips R J N 1980 *Phys. Lett.* B **91** 253
[15] Frixione S and Webber B R 2002 *JHEP* **0206** 029
[16] Frixione S, Nason P and Webber B R 2003 *JHEP* **0308** 007
[17] Nason P 2004 *JHEP* **0411** 040
[18] Frixione S, Nason P and Ridolfi G 2007 *JHEP* **0709** 126